V.M. TRUSOVA,[1] P.E. KUZNIETSOV,[2] O.A. ZHYTNIAKIVSKA,[1] U.K. TARABARA,[1]
K.A. VUS,[1] G.P. GORBENKO[1]

[1] Department of Medical Physics and Biomedical Nanotechnologies,
  V.N. Karazin Kharkiv National University
  (4, Svobody Sq., Kharkiv 61022; e-mail: valerija.trusova@karazin.ua)
[2] O.I. Akhiezer Department for Nuclear Physics and High Energy Physics,
  V.N. Karazin Kharkiv National University
  (4, Svobody Sq., Kharkiv 61022)

FULLERENE-AMYLOID COMPLEXES
AS PERSPECTIVE NANOCOMPOSITES:
MOLECULAR DOCKING STUDIES

The molecular interactions between the amyloid fibrils from $A\beta$-peptide, insulin and α-synuclein and fullerenes of different sizes, including C_{20}, C_{36}, C_{60}, C_{70}, and C_{84}, have been studied using the molecular docking approach. The fullerenes are found to bind to the loop or turn region of $A\beta$- and α-synuclein fibrillar assemblies, but reside at the end of insulin amyloid fibers, reflecting the lower affinity of carbon nanostructures to the latter aggregated protein. For all systems studied here, the fullerene binding to amyloid fibrils is size-dependent, with larger fullerenes exhibiting a higher binding affinity and a lower total energy of complexation. The analysis of side chain contacts highlights the pivotal role of van der Waals forces, specifically, alkyl and π-alkyl interactions, in the stabilization of the fullerene-amyloid complexes. The results obtained are discussed in terms of novel nanocomposite materials based on carbon nanoparticles and fibrillar proteins, as well as of the fullerene role in anti-amyloid therapy.

K e y w o r d s: fullerenes, amyloid fibrils, molecular docking studies, nanocomposite materials.

1. Introduction

According to the theory of the global innovation cycles, the strategical direction of the current progress in science and technology belongs to nanotechnology, a new revolutionary technological paradigm, referring to the material processing on the atomic or molecular scale, especially for the construction of nanoscopic level devices with tunable physicochemical and structural properties [1]. The ability to manipulate the structures at the atomistic resolution allows the design of nanomaterials with unique optical, electrical, mechanical, and magnetic nanoscale characteristics which are currently integrated into a wide range of scientific and industrial areas, including electronics, medicine, biology, information technology, agriculture, just to name a few [2, 3]. To date, a myriad of different engineered nanostructural materials has been produced, which can be catego-

rized into different types either by their origin (inorganic nanomaterials, carbon-based nanomaterials, organic nanomaterials, and composite-based nanomaterials) or their dimensionality (0D, 1D, or 2D assemblies). Among the plethora of the constructed nanostructures, a special attention has been focused on carbon nanomaterials [4]. The carbon-based nanostructures are endowed with extraordinary optical, electrical, chemical, mechanical, and thermal properties, with a promising prospect in different advanced applications such as electronics, batteries, capacitors, wastewater treatment, heterogeneous catalysis, energy storage, imaging, computing, and medical sciences [5, 6]. One prominent class of the carbon-based nanomaterials is represented by fullerenes, or buckyballs, the molecular allotropes of carbon, constituted by a network formed by pentagonal and hexagonal rings forming the sphere-shaped particles [7]. In such a structure, the hybridization state of carbon is sp^2 in which each carbon atom forms three σ-bonds with three other carbon atoms. The extremely high strength, resilience, chemical reactivity along with exceptional optoelectronic and electrochemical properties enable the fullerene application as polymer transistors, photodetectors, sensors, photosensitizers, semiconductors, *etc.* [8]. Along with this, it is anticipated that the size, hydrophobicity, three-dimensionality, and electronic configurations make them an appealing nanoobject for medicinal applications [9]. Their unique carbon cage structure coupled with immense scope for the derivatization make them potential therapeutic agents. Indeed, a number of studies indicate that fullerenes can be employed for antiviral and antibacterial therapies, gene and drug deliveries, bioimaging and medical diagnostics [10]. However, the extensive use of fullerenes in biomedical area faces serious limitations related to the poor biocompatibility, low solubility, and cell toxicity [11]. The hybridization of fullerenes with biopolymers may help to overcome these drawbacks, empowering the broad application of the buckyballs in biomedicine and bionanotechnology. In this respect, the protein fibrillar self-assemblies have emerged as ideal candidates for the conjugation with fullerenes due to their biological compatibility, structural and chemical variabilities, and hierarchically ordered nanostructure [12]. Although amyloid fibrils were traditionally associated with the pathogenesis of different protein misfolding diseases [13], they were

also crowned for their exceptional potential as building blocks for a variety of bionanotechnological areas [14]. A number of recent studies have been devoted to the design of hybridized materials based on amyloid fibrils and carbon nanostructures. Accordingly, Li and Mezzenga successfully conjugated the fibrillar aggregates of β-lactoglobulin and multiwalled carbon nanotubes to generate biocompatible, pH-responsive, and fully brous hydrogels [15]. In turn, Majorošova *et al.* managed to produce the stable colloid nanomaterial composed of lysozyme amyloid fibrils doped with carbon nanotubes [16]. Furthermore, Li and coworkers have fabricated the β-lactoglobulin amyloid fibrils coated with graphene oxide, yielding the biodegradable nanocomposites with shape-memory and enzymatic sensing properties [17]. In the meantime, several studies strongly suggest that fullerenes may inhibit the protein aggregation propensity. Accordingly, using the combination of various experimental techniques, Siposova *et al.* demonstrated the disaggregation impact of fullerenes on the amyloid fibrils of lysozyme and insulin [18]. Based on the extensive atomistic molecular dynamics simulations Liu *et al.* also showed that the binding of fullerenols effectively suppresses the assembly of Aβ-peptide protofibrils [19]. Finally, Bai and co-workers revealed that fullerenes inhibit the β-sheet formation of hI-APP dimer and induce the formation of a collapsed disordered coil-rich peptide configuration [20].

Clearly, the above-mentioned examples allow one to conclude that the pattern of amyloid-buckyball complexes is very intricate, and the stability of the final nanocomposite depends, apparently, on the protein type, fibril morphology, topology, and length, as well as on the experimental conditions. In the present paper, we will make an attempt to gain a further insight into the interactions between fullerenes of different sizes, involving C_{20}, C_{36}, C_{60}, C_{70}, and C_{84}, with fibrillar protein species using the molecular docking technique. The model proteins are represented by the amyloid fibrils from Aβ-peptide, insulin, and α-synuclein.

2. Materials and Methods

2.1. Fullerene structure preparation

The Nanotube Modeler (version 1.8.0) was used for generating the fullerene structures. The Nanotube Modeler is a software tool suitable for modeling
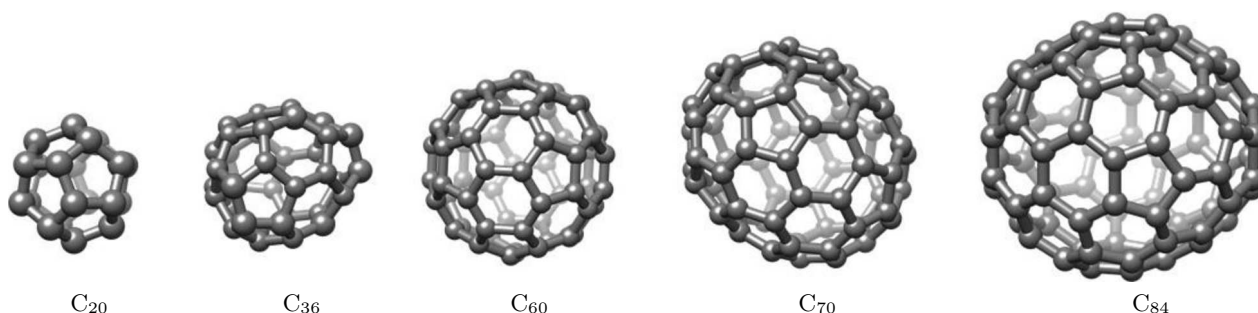
Fig. 1. Chemical structures of fullerenes C_{20}, C_{36}, C_{60}, C_{70}, and C_{84}

and simulating carbon nanotubes and fullerenes. The fullerene structures were specified by inputting the parameters into Nanotube Modeler, including the number of carbon atoms (C_{20}, C_{36}, C_{60}, C_{70}, and C_{84}), type of fullerene, chirality, and symmetry. The generated fullerene structures were validated using the standard techniques such as the energy minimization to ensure its accuracy and reliability.

2.2. Retrieval of protein structures

The three-dimensional X-ray crystal structures of fibrillar Aβ-peptide and α-synuclein were obtained from the Protein Data Bank (https://www.rcsb.org/) using the PDB IDs 2MXU and 2N0A, respectively. The 50-monomer fragment of insulin fibril model was provided by M. Sawaya (http://people.mbi.ucla.edu/sawaya/jmol/fibrilmodels/). All structural models were prepared using the DockPrep module of UCSF Chimera molecular software by removing the heteroatoms, water molecules, and cocrystal ligands, if necessary, and addition of polar hydrogen atoms and Kollman charges [21].

2.3. Molecular docking studies

The blind docking of the fullerene-amyloid complexes was performed using the web-based servers DockThor and HDOCK. The DockThor and HDOCK use different algorithms for the molecular docking. The DockThor employs a rigid-body docking approach which assumes that receptor and ligand maintain their fixed shapes during the docking process [22]. The HDOCK uses a flexible docking approach, allowing for conformational changes of both receptor and ligand during the docking procedure, which may result in more accurate predictions of the binding modes [23]. In addition, the DockThor and HDOCK use different scoring functions to evaluate the binding affinity of the predicted complexes. The scoring functions are used to estimate the strength of the binding between receptor and ligand and are critical for selecting the most promising docking poses. The DockThor employs a physics-based scoring function that considers the factors such as van der Waals interactions, electrostatic interactions, and solvation effects. The HDOCK, in its turn, uses a knowledge-based scoring function that is trained on a large database of experimentally determined protein-ligand complexes. The top-scored docked fullerene-protein complexes were chosen for the subsequent analysis and visualization in BIOVIA Discovery Studio Visualizer, v21.1.0.20298 (San Diego, Dassault Systems, 2021).

3. Results and Discussion

3.1. General characteristics of the examined fullerenes

The structures of the examined fullerenes of different sizes, including C_{20}, C_{36}, C_{60}, C_{70}, and C_{84}, are given in Fig. 1. C_{20} is the smallest fullerene with an icosahedral shape consisting of 20 carbon atoms arranged in a cage-like structure. C_{36}, on the other hand, has a truncated icosahedral shape with 36 carbon atoms forming a closed cage. C_{60} exhibits a spherical shape composed of 60 carbon atoms arranged in a hexagonal pattern, while C_{70} has a slightly elongated shape with 70 carbon atoms forming a combination of hexagonal and pentagonal rings. C_{84} has a more complex structure with additional pentagonal and heptagonal rings, resulting in a non-icosahedral shape. C_{20} is known as the most soluble fullerene, with the highest electron affinity and ionization potential.

C_{60} and C_{70} display similar properties in terms of size, stability, and electronic behavior, while C_{36} pos-
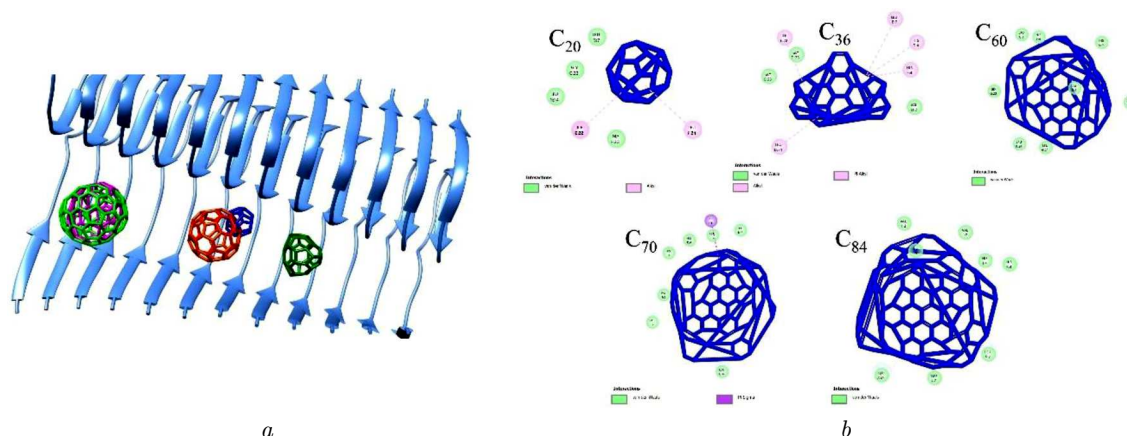
Fig. 2. Docked poses corresponding to the minimum energy (*a*), and 2D plot of binding interactions for the complexes between the fibrillar Aβ-peptide and fullerenes (*b*)
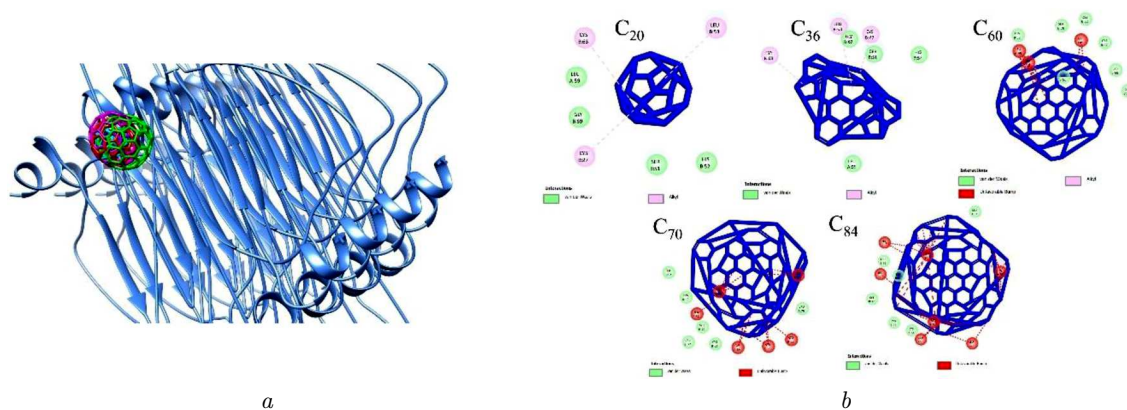

Fig. 3. Location of fullerenes within the insulin amyloid fibrils in the best docking mode (*a*), and side chain contacts in the insulin-fullerene complex (*b*)

sesses characteristics intermediate between C_{20} and C_{60}/C_{70}. C_{84}, and, on the other hand, has a more complex structure with lower solubility and stability, and weaker electron accepting and donating abilities compared to the other fullerenes.

3.2. Molecular docking studies of fullerene-amyloid complexation

To unravel the molecular-level details of the fullerene-amyloid complexation, the molecular docking calculations have been performed using the DockThor and HDOCK servers, followed by the visualization and analysis of the docked complexes in the Discovery Studio. The two servers were used to increase the consistency and reliability of the predictions. The analysis of the docked structures was conducted in terms of

the following characteristics: i) the fullerene location on/within amyloid surface and the interacting amino acid residues, ii) the types of interactions involved in the fullerene-amyloid complexation ensuring the most energetically stable structures.

As seen from Figs. 2–4 (panels *a*), the fullerenes formed stable contacts with the residues present in the loop or turn regions of the Aβ- and α-synuclein fibrils, while, in the case of insulin, all fullerenes are positioned at the end of the amyloid assemblies. Importantly, both the DockThor and HDOCK servers yielded the same positions of fullerenes within the amyloid fibrils under investigation. Such a binding mode ensures the formation of several types of non-covalent contacts, including van der Waals and alkyl/π-alkyl interactions, for all fullerene-amyloid complexes studied here (Figs. 2–4, panels *b*). No-
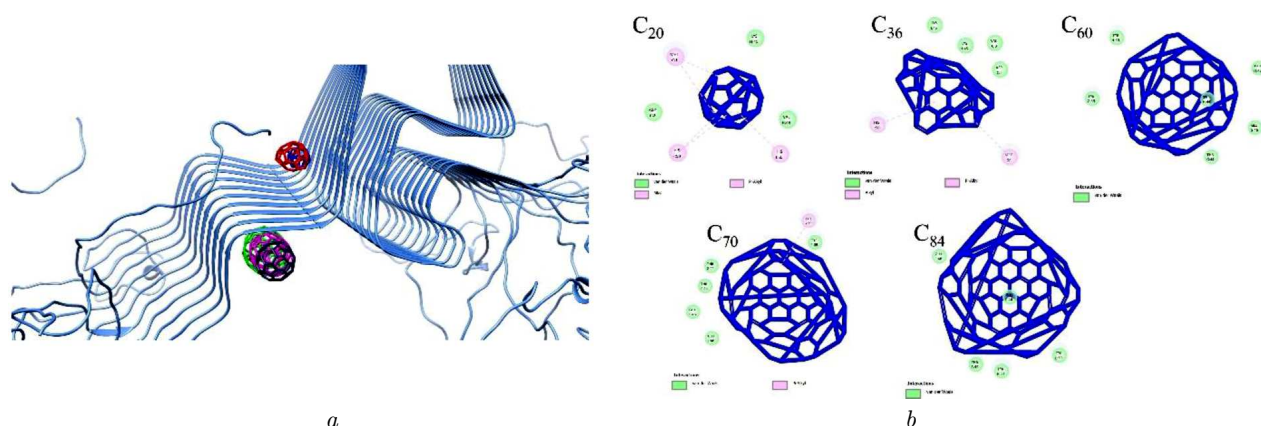
Fig. 4. 3D (*a*) and 2D (*b*) structures of α-synuclein amyloid fibrils docked with fullerenes

tably, the association of the carbon nanoparticles with the insulin fibers was stabilized also by unfavorable bump interactions. As generally known, van der Waals interactions are weak attractive forces that arise from fluctuations in the electron density within molecules [24].

In the case of complexes between fullerenes and amyloid fibrils, van der Waals interactions occur between the surfaces of the interacting molecules. The fullerenes, which are large, hollow, cage-like structures made of carbon atoms, have a unique shape that allows them to interact with the exposed hydrophobic regions of amyloid fibrils, composed of misfolded proteins. The van der Waals forces between the fullerenes and the hydrophobic amino acid residues of the amyloid fibrils lead to the stabilization of the complex by providing attractive forces that help to overcome the repulsive electrostatic interactions between the fullerenes and the charges present on amyloid side chain. The alkyl interactions are generally defined as non-covalent interactions between hydrophobic alkyl groups. The fullerenes, which have many alkyl groups on their surface, can form alkyl contacts with the hydrophobic side chains of amino acid residues in the amyloid fibrils [25]. The alkyl groups in the fullerenes interact with the hydrophobic amino acid residues through van der Waals forces and hydrophobic interactions, leading to the stabilization of the complex. The alkyl interactions are important in maintaining the structural integrity of the complex and preventing the dissociation of the fullerenes from the amyloid fibrils. Finally, the π-alkyl interactions are non-covalent interactions that occur between the π-

electron cloud of an aromatic ring and the alkyl group of another molecule [26]. The fullerenes, which have multiple aromatic rings on their surface, can form π-alkyl contacts with the aromatic amino acid residues of the amyloid fibrils, such as phenylalanine, tyrosine, and tryptophan. The π-electron cloud of the aromatic rings in the fullerenes interacts with the alkyl group of the aromatic amino acid residues through van der Waals forces and π-alkyl interactions, leading to the stabilization of the complex. The π-alkyl interactions are important for enhancing the binding affinity, as they provide additional attractive forces that contribute to the overall stability of the complex. Special attention should be paid to the discussion of unfavorable bump interactions found only in the insulin-fullerene complexes. The unfavorable bump interactions refer to steric clashes or clashes in van der Waals radii between molecules, resulting in repulsive forces due to the overlap of their electron clouds. These interactions can occur, when two molecules come into close proximity, and their three-dimensional structures do not allow for a proper fit, leading to the repulsion and hindrance of molecular interactions. The finding that unfavorable bump interactions are formed only in the case of fibrillar insulin can be attributed to the following factors:

1. *size and shape*: the fullerenes are cage-like structures composed of carbon atoms, with a highly symmetrical structure. The insulin amyloid fibrils, on the other hand, are elongated protein aggregates with a complex hierarchical structure. The size and shape of fullerenes may lead to unfavorable bump interactions with the protein molecules within the insulin amy-

Table 1. **Amino acid residues participating in the formation
of fullerene-amyloid complexes. N_C is the number of side-chain contacts
between the fibrils and fullerenes. The last letter in the amino acid code refers to the chain
of the fibril. Given in Italic bold are the amino acids forming unfavored bump interactions**

Protein	Fullerene	N_C	Amino acid residues forming a contact with fullerene
$A\beta$	C_{20}	6	Leu27-G, Gly23-G, Leu24-G, Ile22-G, Gly23-F, Leu24-F
	C_{36}	8	Ile22-G, Gly23-D, Gly23-E, Leu24-D, Val2-D, His4-E, His4-D, Leu7-E
	C_{60}	8	Leu7-G, His4-F, His4-G, Val2-G, Val2-F, Leu24-G, Leu24-F, Gly23-G
	C_{70}	8	His4-I, Val2-J, Val2-I, Leu24-J, His4-K, Leu7-J, His4-J, Leu7-K
	C_{84}	8	Val2-I, His4-I, Val2-J, His4-J, His4-K, Leu7-K, Leu7-J, Leu24-J
Insulin	C_{20}	7	Cys68-B, Leu59-A, Gly69-B, Cys27-B, Ser51-B, His52-B, Leu53-B
	C_{36}	7	Cys68-B, Leu53-B, Gly69-B, Cys27-B, Ser51-B, His52-B, Leu59-A
	C_{60}	10	His52-B, Ser70-B, Cys32-B, Cys27-B, Cys68-B, Cys28-B, Ser51-B, ***Leu53-B, Leu59-A, Gly69-B***
	C_{70}	12	Ser12-B, His52-B, Cys32-B, Ser70-B, Cys27-B, Leu78-A, ***Ser51-B, Leu53-B, Gly69-B, Cys68-B, Cys28-B, Leu59-A***
	C_{84}	13	Leu57-A, Leu72-B, Ser51-B, Cys32-B, Cys27-B, Cys28-B, ***His52-B***, ***Ser70-B, Leu53-B, Leu59-A, Gly69-B, Cys68-B, Leu78-A***
α-synuclein	C_{20}	6	Met1-C, Asp2-C, His50-H, His50-I, Val48-H, Lys45-H
	C_{36}	6	His50-I, Lys45-I, Lys45-H, Val3-C, Asp2-C, Met1-C
	C_{60}	6	Tyr39-H, Tyr39-G, Thr44-G, Thr44-H, Glu46-G, Glu46-H
	C_{70}	6	Thr44-G, Thr44-F, Glu46-G, Glu46-F, Tyr39-F, Tyr39-G
	C_{84}	5	Glu46-F, Glu46-E, Tyr39-E, Tyr39-F, Thr44-F

loid fibrils, as the large size and cage-like structure of fullerenes may clash with the elongated structure of the fibrils. In contrast, $A\beta$- or α-synuclein amyloid fibrils may have a different conformations and surface architectures that allows for a better fit with the fullerenes, thereby reducing the occurrence of unfavorable bump interactions. These considerations are confirmed by the fact that fullerenes accommodate within the interior of $A\beta$- or α-synuclein fibers, but do not actually dock into the insulin fibrillar aggregates;

2. *surface properties*: the surface of fullerenes is highly hydrophobic, while the surface of amyloid fibrils can have both hydrophobic and hydrophilic regions. The hydrophobic nature of the fullerenes may lead to unfavorable bump interactions with the hydrophobic regions of the insulin amyloid fibrils, which can further disrupt the fibril structure. On the other hand, the surface properties of $A\beta$- or α-synuclein amyloid fibrils may be different, with less hydrophobicity or a different distribution of hydrophobic and hydrophilic regions, resulting in the absence of unfavorable bump interactions with the fullerenes;

3. *morphological and surface properties of amyloid fibrils*: The amyloid fibrils from the insulin,

$A\beta$- and α-synuclein, have distinct morphologies and surface characteristics. These differences may affect the likelihood of unfavorable bump interactions with the fullerenes. For example, the $A\beta$- and α-synuclein amyloid fibrils have been reported to have a more compact and less elongated structure compared to the insulin amyloid fibrils [27], which may result in a better fit with fullerenes and reduced occurrence of unfavorable bump interactions.

The amino acid residues, which are in contact with the amyloid fibers, involve mainly Leu, His, Gly, and Val. In the case of α-synuclein, Tyr, Thr, Lys, Met also participate in the stabilization of the fullerene-amyloid complexes (Table 1). Overall, as shown in Table 1, the fullerenes form from 5 to 13 contacts with the fibrillar proteins. Notably, no strong correlation between the number of contacts and fullerene size was found.

Table 2 shows the comparison of the numerical results for the fullerene-amyloid molecular docking. Although both docking servers are used for blind protein-ligand docking, one of the major differences between them is the output parameters they provide. The DockThor gives the information about the en-

ergy of interaction and the binding affinity. The total energy of binding refers to the sum of all energy contributions that stabilize the docked complex. This includes van der Waals interactions, electrostatic interactions, hydrogen bonds, and desolvation effects. The binding energy can be calculated as the difference between the energy of the docked complex and the energy of the individual ligand and receptor molecules in their unbound state. The HDOCK, in its turn, provides a single docking score that reflects the overall quality of the predicted complex. The docking score is a measure of the quality of the predicted complex and reflects how well the docked poses fit together. It accounts for the factors such as the shape complementarity of the binding interface, the number of intermolecular contacts, and the energy of the complex. The higher the docking score, the better the predicted complex is considered to be.

Nonetheless, as seen from Table 2, both the DockThor and HDOCK yield the same tendencies in the binding pattern for all complexes studied here. Specifically, the total binding energy and docking score were found to decrease with the fullerene size, while the binding affinities were shown to enhance in the region from C_{20} to C_{84}. This means that larger fullerenes have a higher affinity for amyloid fibrils and exhibit a stronger binding. Additionally, larger fullerenes may have a larger surface area and more binding sites that can interact with the amyloid fibrils, which is reflected in a strong correlation between the strength of binding and the fullerene size. Finally, larger fullerenes have a higher tendency to form clusters or aggregates, which can enhance their binding to amyloid fibrils. Another noteworthy observation is that the contribution of van der Waals interactions in the total energy of binding also shows a strong correlation with the fullerene size highlighting the pivotal role of non-covalent interactions in the stabilization of the fullerene-amyloid complexes. Importantly, our results are in a perfect agreement with the results reported previously by Huy and Li [28]. Accordingly, the authors also showed that the size of fullerenes plays an important role in the control over their association with the protein fibrillar assemblies.

In conclusion, our molecular docking results show that the fullerenes readily bind to the interior of the $A\beta$- and α-synuclein amyloid fibrils, but reside at the ends of the insulin fibrillar aggregates. In all cases, it is found that the total energy of binding de-

creases, while the binding affinity increases linearly with the fullerene size. The analysis of the side chain contacts revealed the key role of van der Waals interactions in the stabilization of the amyloid-fullerene complexes. These findings may have several potential applications. First, the obtained results highlight the possibility of creating the novel composite nanomaterials based on the fullerenes and amyloids with unique properties. For example, the electronic properties of fullerene molecules, such as their high electron affinity and ability to act as an electron acceptor, make them attractive for applications in electronics and optoelectronics. When combined with amyloid, which can provide the structural stability and biocompatibility, the fullerenes can be used to develop organic electronic devices such as photovoltaics, light-emitting diodes, and field-effect transistors. Other areas, where such nanocomposites may find applications, include drug delivery, tissue engineering, sensing, and environmental protection. On the other hand, in view of the fullerene ability to serve as therapeutic agents for neurodegenerative diseases by the selective targeting and binding to amyloid fibrils, our data may create a basis for a better understanding of the molecular mechanisms of the

Table 2. **Comparison of the molecular docking results of fullerene-amyloid complexes obtained with the DockThor or HDOCK servers**

Protein	Fullerene	DockThor			HDOCK
		Affinity	Total energy	vdW energy	Docking score
$A\beta$	C_{20}	−8.32	−22.14	−17.63	−69.02
	C_{36}	−10.21	−94.62	−28.65	−112.38
	C_{60}	−11.86	−154.31	−29.21	−146.88
	C_{70}	−12.14	−178.63	−31.48	−165.96
	C_{84}	−14.72	−192.88	−34.02	−172.97
Insulin	C_{20}	−8.24	−22.09	−17.31	−99.73
	C_{36}	−8.32	−95.17	−18.12	−112.87
	C_{60}	−8.36	−162.31	−19.08	−145.70
	C_{70}	−8.37	−203.95	−20.29	−162.71
	C_{84}	−8.46	−260.83	−21.35	−174.27
α-synuclein	C_{20}	−8.11	−24.03	−15.71	−95.97
	C_{36}	−8.75	−106.28	−22.99	−129.63
	C_{60}	−9.16	−162.31	−29.08	−139.48
	C_{70}	−9.38	−203.94	−30.29	−143.72
	C_{84}	−9.45	−260.83	−31.35	−152.58

fullerene-based anti-amyloid strategies. The fgbfnur-ther careful research is strongly required to clarify the role of fullerene derivatives in the anti-amyloid applications.

1. A. Cho, S. Park. Exploring the global innovation systems perspective by applying openness index to national systems of innovation. *J. Open Innov. Technol. Mark. Complex* **8**, 181 (2022).

2. P.K. Sharma, S. Dorlikar, P. Rawat, V. Malik, N. Vats, M. Sharma, J.S. Rhyee, A.K. Kaushik. *Nanotechnology and its application: A review* (Nanotechnology in Cancer Management, 2021).

3. H. Mobeen, M. Safdar, A. Fatima, S. Afzal, H. Zaman, Z. Mehdi. Emerging applications of nanotechnology in context to immunology: A comprehensive review. *Front. Bioeng. Biotechnol.* **10**, 1 (2022).

4. A.D. Goswami, D.H. Trivedi, N.L. Jadhav, D.V. Pinjari. Sustainable and green synthesis of carbon nanomaterials: A review. *J. Environ. Chem. Engineer.* **9**, 106118 (2021).

5. R. Sridharan, B. Monisha, P.S. Kumar, K.V. Gayathri. Carbon nanomaterials and its applications in pharmaceuticals: A brief review. *Chemosphere* **294**, 133731 (2022).

6. R.B. Onyancha, K.E. Ukhurebor, U.O. Aigbe, O.A. Osibote, H.S. Kusuma, H. Darmokoesoemo. A methodical review on carbon-based nanomaterials in energy-related applications. *Ads. Sci. Technol.* **2022**, 4438286 (2022).

7. P. Harris. Fullerene polymers: A brief review. *J. Carbon Res.* **6**, 71 (2020).

8. M. Paukov, C. Kramberger, I. Begichev, M. Kharlamova, M. Burdanova. Functionalized fullerenes and their applications in electrochemistry, solar cells, and nanoelectronics. *Materials* **16**, 1276 (2023).

9. R. Bakry, R.M. Vallant, M. Najam-ul-Haq, M. Rainer, Z. Szabo, C.W. Huck, G.K. Bonn. Medicinal applications of fullerenes. *Int. J. Nanomedicine* **2**, 639 (2007).

10. H. Kazemzadeh, M. Mozafari. Fullerene-based delivery systems. *Drug Discovery Today* **24**, 898 (2019).

11. N. Malhotra, G. Audira, A.L. Castillo, P. Siregar, J. Ruallo, M.J. Roldan, J.-R. Chen, J.-S. Lee, T.-R. Ger, C.-D. Hsiao. An update report on the biosafety and potential toxicity of fullerene-based nanomaterials toward aquatic animals. *Oxid. Med. Cell Longev.* **2021**, 7995223 (2021).

12. C. Li, R. Mezzenga. The interplay between carbon nanomaterials and amyloid fibrils in bio-nanotechnology. *Nanoscale* **5**, 6207 (2013).

13. P.C. Ke, R. Zhou, L.C. Serpell, R. Riek, T.P.J. Knowles, H.A. Lashuel, E. Gazit, I.W. Hamley, T.P. Davis, M. Fandrich, D.E. Otzen, M.R. Chapman, C.M. Dobson, D.S. Eisenberg, R. Mezzenga. Half a century of amyloids: past, present and future. *Chem. Soc. Rev.* **49**, 5473 (2020).

14. B. Choi, T. Kim, S.W. Lee, K. Eom. Nanomechanical characterization of amyloid fibrils using single-molecule experiments and computational simulations. *Nanoscale Biol. Mater.* **2016**, 5873695 (2016).

15. C. Li, R. Mezzenga. Functionalization of multiwalled carbon nanotubes and their pH-responsive hydrogels with amyloid fibrils. *Langmuir* **28**, 10142 (2012).

16. J. Majorošova, M.A. Schroer, N. Tomašovičová, M. Batková, P.-S. Hu, M. Kubovčíková, D.I. Svergun, P. Kopčanský. Effect of the concentration of protein and nanoparticles on the structure of biohybrid nanocomposites. *Biopolymers* **111**, e23342 (2020).

17. C. Li, J. Adamcik, R. Mezzenga. Biodegradable nanocomposites of amyloid fibrils and graphene with shape-memory and enzyme-sensing properties. *Nat. Nanotechnol.* **7**, 421 (2012).

18. K. Siposova, V.I. Petrenko, O.I. Ivankov, A. Musatov, L.A. Bulavin, M.V. Avdeev, O.A. Kyzyma. Fullerenes as an effective amyloid fibrils disaggregating nanomaterial. *ACS Appl. Mater. Interfaces* **12**, 29 (2020).

19. Z. Liu, Y. Zou, Q. Zhang, P. Chen, Y. Liu, Z. Qian. Distinct binding dynamics, sites and interactions of fullerene and fullerenols with amyloid-β peptides revealed by molecular dynamics simulations. *Int. J. Mol. Sci.* **20**, 2048 (2019).

20. C. Bai, Z. Lao, Y. Chen, Y. Tang, G. Wei. Pristine and hydroxylated fullerenes prevent the aggregation of human islet amyloid polypeptide and display different inhibitory mechanisms. *Front. Chem.* **8**, 51 (2020).

21. E. Pettersen, T. Goddard, C. Huang, G. Couch, D. Greenblatt, E. Meng, T. Ferrin. UCSF Chimera – a visualization system for exploratory research and analysis. *J. Comput. Chem.* **25**, 1605 (2004).

22. I. Guedes, A.M.S. Barreto, D. Marinho, E. Krempser, M.A. Kuenemann, O. Sperandio, L.E. Dardenne, M.A. Miteva. New machine learning and physics-based scoring functions for drug discovery. *Sci. Rep.* **11**, 3198 (2021).

23. Y. Yan, D. Zhang, P. Zhou, B. Li, S.-Y. Huang. HDOCK: A web server for protein–protein and protein–DNA/RNA docking based on a hybrid strategy. *Nucl. Acids Res.* **45**, W365 (2017).

24. M. Karplus, H. J. Kolker. Van der Waals forces in atoms and molecules. *J. Chem. Phys.* **41**, 3955 (1964).

25. R. Macovez. Physical properties of organic fullerene cocrystals. *Front. Mater.* **4**, 46 (2018).

26. J. Ribas, E. Cubero, F. Luque, M. Orozco. Theoretical study of alkyl-π and aryl-π interactions. Reconciling theory and experiment. *J. Org. Chem.* **67**, 7057 (2002).

27. Y. Li, C. Zhao, F. Luo, Z. Liu, X. Gui, Z. Luo, X. Zhang, D. Li, C. Liu, X. Li. Amyloid fibril structure of α-synuclein determined by cryo-electron microscopy. *Cell Res.* **28**, 897 (2018).

28. P. Huy, M. Li. Binding of fullerenes to amyloid beta fibrils: size matters. *Phys. Chem. Chem. Phys.* **16**, 20030 (2014).

В.М. Трусова, П.Е. Кузнєцов,
О.А. Житняківська, У.К. Тарабара,
К.О. Вус, Г.П. Горбенко

КОМПЛЕКСИ ФУЛЕРЕНІВ З АМІЛОЇДНИМИ ФІБРИЛАМИ ЯК ПЕРСПЕКТИВНІ НАНОКОМПОЗИТИ: ДОСЛІДЖЕННЯ МЕТОДОМ МОЛЕКУЛЯРНОГО ДОКІНГУ

Молекулярні взаємодії між амілоїдними фібрилами $A\beta$-пептиду, інсуліну та α-синуклеїну та фулеренами різного розміру, зокрема, C_{20}, C_{36}, C_{60}, C_{70} та C_{84}, було досліджено за допомогою методу молекулярного докінгу. Виявлено, що фулерени зв'язуються з петлями або поворотами фібрилярних агрегатів $A\beta$-пептиду та α-синуклеїну, але локалізуються на кінцях амілоїдних фібрил інсуліну, що свідчить про нижчу спорідненість фулеренів до білкових агрегатів цього типу. Для всіх систем, досліджених у даній роботі, зв'язування фулеренів з амілоїдними фібрилами залежало від розміру, причому більші фулерени проявляли вищу афінність та меншу загальну енергію комплексації. Аналіз контактів бічних ланок підкреслив ключову роль ван-дер-Ваальсових сил, зокрема, алкільних та π-алкільних взаємодій, в стабілізації комплексів фулерен-амілоїд. Отримані результати було обговорено у контексті нових нанокомпозитних матеріалів на основі вуглецевих наночастинок та фібрилярних білків, а також ролі фулеренів в антиамілоїдній терапії.

К л ю ч о в і   с л о в а: фулерени, амілоїдні фібрили, молекулярний докінг, нанокомпозитні матеріали.